

Feasibility of MEMS Hollow Cathode Devices for Micro-Spacecraft Plasma Propulsion

Angelo N. GRUBISIC

Doctoral Researcher, Astronautics Research Group, University of Southampton

Andy CRANNY

School of Electronics and Computer Science, University of Southampton

Stephen B. GABRIEL

Head of Astronautics Research Group, University of Southampton

Micro-satellites in the 1-20kg range with limited onboard resources would benefit greatly from miniaturized, low power electric propulsion systems. This paper reports on a feasibility study into the scaling and application of MEMS manufacturing techniques to produce such a micro-hollow cathode thruster.

Keywords: Hollow cathode, propulsion, micro, pico, spacecraft, plasma, thruster

Nomenclature

α	= Degree of ionization
A	= Area, m ²
amu	= Atomic mass unit
d	= Diameter, m
ϵ_i	= Ionization potential, eV or Emissivity
e	= Electron charge, C
E	= Electric field, V/m
f	= View factor
I	= Current, A
J	= Current density, A/m ²
k	= Boltzman's constant, 1.381×10^{-23} J/K
L	= Characteristic length, m
m	= Particle mass, kg
\dot{m}	= Mass flow rate, kg/s
n	= Particle density, m ⁻³
p	= pressure, N/m ²
P	= Power, W
q_r	= Radiative heat flux, W
r	= Radius, m
R	= Resistance, Ohms
R_{xe}	= Molar gas constant for xenon
T	= Temperature, K
V	= Potential, V
η	= Plasma resistivity, Ohm/m
λ_d	= Debye length, m
$\ln A$	= Coulomb logarithm
V_p	= Plasma potential, V
v	= Velocity, m/s
σ	= Conductivity, Ohms/m or Stefan constant
γ	= Ratio of specific heats (5/3 for xenon)

Subscripts

A	= Anode
n	= Neutrals
c	= Cathode
D	= Discharge current
d	= Debye
$ds1,2$	= Double sheath at orifice entrance and exit
e	= Electrons
eq	= Equivalent
ex	= Exit
eff	= Effective
em	= Emitter
f	= Fall
h	= Heater
i	= Ions
ins	= Emitter
oh	= Ohmic
o	= Orifice
p	= Plasma
s	= Static
th	= Thermionic

1. Introduction

Recently at the University of Southampton, a new form of thruster termed the hollow cathode thruster (HCT) has been researched based on the T5 and T6 hollow cathodes [1-5]. These particular cathodes are a mature technology developed extensively over the last 35-years for

application on the UK-10, UK-25, T5 and T6 gridded ion thrusters [6-11] and as an electron source for various ion beam neutralisation applications [12]. By reducing orifice diameter of cathodes to enhance Ohmic heating as in the T5 hollow cathode, thrust efficiencies over 16% are achieved. This mode of operation is similar to a low power (<80W), diffuse discharge thermal arcjet. In this case, thrusts in the milli-Newton range can be generated with specific impulse of over 400s with argon.

T5 HC may present a microthruster suitable for smaller satellites (<150kg) which have typically relied on only the simplest propulsion systems due to the severe resource constraints (power, regulation, mass, volume, cost) on small spacecraft. In particular, satellites in the 1-20kg range have even greater restriction on their propulsion systems and would benefit the most from development of a higher performance low power electrothermal thruster.

The advent of MEMS (micro-electro-mechanical-systems) technologies particularly for the plasma display industry have been identified as a possible means to build highly miniaturised low power (0.1-5W) on-chip electrothermal propulsions systems suitable for relatively high performance. A representative subsystem is shown in Figure 1.

2. Operating Principle

In this application of hollow cathodes for electric propulsion applications, a tungsten filament heater is used to raise the temperature of a thermionic emitter (>1000°C) sufficient for initial emission. A trigger voltage applied to an external electrode is typically used to initiate the discharge (15-200V). The orifice plate increases the internal pressure and generates sufficiently dense plasma within the internal volume to promote ion recombination at the emitter surface and the hollow cathode effect itself. Self-heating is then maintained by the acceleration of ions through the sheath (region between the cathode emitter and plasma column), which recombine on internal surfaces to form neutrals.

The plasma column induces sheath-enhanced emission at the emitter surface due to the intense field ($\sim 10^7$ V/m) between the plasma column and cathode emitter potentials at a distance on the order of the Debye length. The emitter is manufactured from lanthanum hexaboride (LaB_6) which slowly evaporates and dissociates to produce work function lowering compounds at the emitter surface corresponding to a decrease in effective work function [13].

Thermionically emitted electrons are accelerated through the sheath potential and generally considered as a mono-energetic beam. The hollow cathode effect is the process of emission of electrons through the sheath perpendicular to the cathode which are then repulsed by the same sheath on the opposing side of the emitter hereby containing the high energy electrons within the cavity and enabling a greater number of electron-ion collisions within the plasma than in conventional planar discharges. Since the path length of electrons is increased and the voltage required to sustain the discharge dramatically drops as the current is increased resulting in a negative differential resistance characteristic and is distinctive of the hollow cathode mode. The plasma potential within the emitter volume generally remains 6-10V above the cathode potential consistent with the energy required for the excitation of meta-stable states of xenon (3P0 \sim 9.45eV, 3P2 \sim 8.32eV). Ion production is generally assumed to be achieved by multi-step processes firstly by electron impact of primary electrons from the atomic ground state [14] within the emitter volume, and then by lower energy thermalized electrons (2-4eV) within the orifice which then contribute significantly to the ionisation process. The total process thus requires transfer of at least the ionisation energy (12.13eV for xenon). The discharge current is drawn through the orifice toward the anode. Processes within the orifice generally dominate performance. The operating regime acts to maintain emitter temperatures for thermionic emission by balancing power deposition to the cathode with cooling by particle efflux and heat transfer to the surroundings. Energy input to the plasma can be attributed to the energy of thermionically emitted electrons accelerated through the cathode fall and through Ohmic (collisional) heating within the orifice channel.

3. Thrust Mechanism and Model

The study considered 3 small spacecraft configurations with associated mass and inertial characteristics. Spacecraft of 1kg, 10kg and 20kg mass are shown to require minimum thrust levels of 0.014mN, 0.043mN and 0.11mN respectively for a 10-second impulsive burn either side of a slew period of either 20 or 100s. These are shown in Table 1. The full study designed both a conservative and ambitious system for each configuration however in this overview we shall consider only the conservative design for the 20kg satellite to explore the required terminal and geometric parameters of such a device. Since small impulse times are at least, at present limited, impulsive burn periods are assumed to be over 10-seconds per burn.

The MEMS manufacturing process only allows for the constriction of a simple constrictor like orifice. The thrust contribution at the orifice exit in this case will consist of components of momentum and pressure thrust given by:

$$F = \dot{m} \sqrt{\gamma R_{xe} T_i} + A_{or} (n_e k T_e + n_i k T_i + n_n k T_n) \quad (3.1)$$

This assumes that the flow leaves the orifice at the acoustic velocity based on a choked flow approximation which is a fair based on flow into a hard vacuum and the high pressure of the discharge. For the full description of the model the reader referred to the feasibility study however an overview is given here. Since the emitter temperature profile is not constant along the length of the cathode, integrals allow for the resulting variation in current density from the emitter. Electron emission provides energy to the plasma in the form of electrons accelerated by the cathode fall. This energy is utilised to ionise and excite the gas, and heat the plasma electrons. Energy is also added to the plasma by Ohmic heating of the resistive plasma within the orifice. Energy is lost by particles flowing out of the cathode, given by:

$$\int J_{th} \left(V_p + \frac{5kT_e}{2e} \right) dA_{em} + \int \frac{J_D^2}{\sigma} dV = \int J_i \left(\varepsilon_i + \frac{5kT_i}{2e} \right) dA_s + \int J_e \left(\frac{5kT_e}{2e} \right) dA_s + (I_D + \alpha I_{eq}) \left(\frac{5kT_e}{2e} \right) + \frac{I_{eq}}{\alpha} \left(\frac{5kT_e}{2e} \right) + q_r \quad (3.2)$$

Energy balance is a result of resistive heat input into the orifice, and electrons accelerated through the sheath potential. Assuming negligible radiative losses, and conventional energy equipartition theorem yields an expression for the power loss by particle efflux and ion recombination as:

$$P_{loss} = J_i \varepsilon_i \pi r (r + 2l) \left(\frac{5kT_e}{2e} \right) + I_D \left(\frac{5kT_e}{2e} \right) \quad (3.3)$$

Orifice resistance is approximated to that of a fully ionised gas due to the high degree of ionisation [15]. Electron temperature is generally 0.5-2eV within the orifice with a plasma density $\sim 1 \times 10^{22} \text{m}^{-3}$. The total discharge current is based on the contributions of all particle fluxes at the cathode surface for preservation of current continuity and is expressed as:

$$I_D = I_{th} + I_i - I_e \quad (3.4)$$

The total discharge voltage can be expressed as:

$$V_d = V_p + \Delta V_{ds1} + \Delta V_{oh} + \Delta V_{ds2} \quad (3.5)$$

This is the sum of the cathode fall voltage, the Ohmic drop across the orifice and the double sheaths at the entrance and exit of the orifice. Typical operating power for the microthrusters is in the 0.1-3W range. The plasma pressure in the hollow cathode orifice can be evaluated from the equation of state:

$$p_s = n_e k T_e + n_i k T_i + n_n k T_n \quad (3.6)$$

Typical flow rates are in the 0.1-0.4mgs⁻¹ range. The internal pressure may, as a first approximation, be estimated from the critical flow relation for sonic flow through the orifice assumed to be adiabatic.

$$p_{em} = p_{or} \left(1 + \frac{\gamma - 1}{2} \right)^{-1/(\gamma - 1)} \quad (3.7)$$

At the emitter surface, the energy loss due to convected thermionic electrons is balanced primarily by ion bombardment. The energy balance can be expressed as:

$$\int J_{th} \left(\phi_{eff} + \frac{5kT_c}{2e} \right) dA_e = \int J_i (\varepsilon_i + V_f - \phi_{eff}) dA_e \quad (3.8)$$

This then allows the calculation of the required emitter temperature based on the contribution of all particle fluxes to the surface. Heat is deposited in the anode primarily by electron convection and ion bombardment. To avoid anode overheating, and assuming the anode is cooled radiatively the necessary anode area required for a given heat input to maintain a given temperature is given by:

$$A_a = \frac{1}{\varepsilon_a [T] \sigma T_a^4} I_D \left(\frac{5kT_e}{2e} \right) \quad (3.9)$$

Assuming that the resistive heating element has reasonable dimensions, heater resistance is given by:

$$R_h = \frac{\rho_h [T_h] L_h}{A_h} \quad (3.10)$$

Assuming negligible conductive heat transfer the energy balance between the heater input power and power radiated by the cathode is given by:

$$I_h^2 R_h = A_c \varepsilon_c [T] \sigma T_c^4 \quad (3.11)$$

For application to small satellites is necessary to base heater design for operation from a 24V bus able to provide current regulation.

4. Propellant Selection

Lighter propellants generate higher specific impulse however the properties of xenon make it attractive for small satellite applications, which are generally more volume limited rather than mass limited. This makes the density-Isp (the product of the specific impulse and the propellant density) much higher than other inert propellants. The low primary ionisation energy of xenon, in comparison to all other inert gases, also minimises the reduction in efficiency due to ionisation losses (a form of frozen flow loss) in the propellant also resulting in lower discharge voltages. Characteristics of the propellants considered are shown below in Table 2.

5. Electrical Breakdown and Oscillatory Enhancement

It has been shown that field-emission-related effects play a significant role in the deviation of the breakdown voltage from that predicted by Paschen's law in the range of micrometer gaps and supports avalanche breakdown. [16] Inclusion of field emission causes the rapid fall of the breakdown voltage indicating that breakdown is no longer controlled by the processes within the gas. At the gas pressure of 760 torr or higher, the electron mean path is of the order of a few micrometers so at small inter-electrode spacing breakdown is initiated by secondary-emission processes.

Micro-hollow cathode discharges are not an extension of the low-pressure discharges to higher pressures since their observed stable operation at cathode openings of 250µm at atmospheric pressure violates the “White-Allis” similarity law which relates the sustaining voltage of discharges is dependent on the product of gas pressure and electrode separation [17, 18]. Low voltage high-pressure operation of a HC discharge can be accomplished by reducing the size of the emitter cavity to maintain a hollow cathode effect as discussed previously.

Microdischarges can be operated in parallel without individual ballast resistors, if the discharges are operated in the range where the current-voltage ($I-V$) curve has a

positive slope [19-23]. In regions where the $I-V$ characteristics have a negative slope (hollow cathode mode) or is flat (normal glow mode), arrays can be generated by using a distributed resistive ballast such as semi-insulating silicon as the anode material [24] or multilayer ceramic structures where each microdischarge is individually ballasted typically with a 3.96kΩ load [25, 26]. One alternative is to operate in the pre-hollow cathode discharge mode or in the abnormal glow mode [27]. However, this represents a specific operating point and is thus likely to constrain the thrust range of any particular device unless some form of device switching is included, which brings about additional considerations such as discrete feed and electrical systems. The initial concept nevertheless is a device with a single operating point.

The supporting micro-flow valve technologies have also been under development such as micro-piezoelectric actuators at the University of Uppsala [28] and micro-isolation valves at JPL [29]. The University of Southampton also has experience in fabricating such building blocks and microfluidic chips such as micro-machined pumps suitable for pumping gaseous media [30-32] integrated microfluidic circuit boards [33] and actuators that are suitable for valves [34].

6. Emitter Selection

Emitting materials such as LaB₆ and CeB₆ slowly evaporate during operation to produce the work function lowering compounds. LaB₆ has been extensively used in the Russian electric propulsion program and has demonstrated reliable operation for thousands of hours [35]. Due to their higher work function ~2.6eV the power required for the same current levels are higher. However, since the work function lowering compound in LaB₆ and CeB₆ cathodes is the emitter itself, no impregnation, activation or post process machining is required during construction. As a consequence, boride emitters could possibly be directly manufactured by MEMS processes or micromachining into a boride substrate presenting significant simplification of the manufacturing problem when compared to impregnated cathodes. Lanthanum hexaboride hollow cathodes are also two orders of magnitude less sensitive to emitter poisoning than impregnated cathodes. As a consequence, this design studies considers LaB₆ the quintessential emitter material for this purpose.

7. Manufacturing Methods

The basic design is composed of two electrically conductive sections (the cathode and anode) separated by an insulating layer. At least one of these conductive sections, preferably the anode, would be fabricated in electrically conductive silicon (p-type or n-type). There is also a choice in the composition of the insulating layers, which can be produced from a number of different silicides (e.g. silicon dioxide, silicon nitride or silicon carbide). Taking the silicon on insulator fabrication route as an example and taking into consideration the conventional silicon processing techniques such as photolithography (subtractive/additive pattern transfer), subtractive processes (wet etching, dry etching, milling) additive Processes (chemical vapour deposition, physical vapour deposition, thermal oxidation, sol-gel deposition, spin coating, ion implantation, electrochemical deposition) and bonding (anodic bonding, direct bonding, eutectic bonding, adhesive bonding) processes available a number of generic micro-scaled structures can be imagined, as shown in Appendix 1. In formulating these designs, three binary-weighted design options have been included, namely forming the thruster nozzle by an anisotropic etching method (slanted sidewalls, square profile) or by a deep reactive ion etching method (straight sidewalls, circular profile); the inclusion or absence of a 'chimney' structure within the thruster nozzle; the inclusion or absence of an orifice at the hollow cathode end-plate. Each of these generic designs has relative merits and shortcomings that effect different aspects of the system as a whole.

The School of Electronics and Computer Science at Southampton University, MEMS fabrication techniques have been used to realise similar devices. It is likely that the future will see the development of arrays with smaller apertures possibly down to $1\mu\text{m}$ in diameter. Micromanufacturing has also shown it is possible to separate power feeds to the anodes of groups of 3×3 arrays as [36].

Wang *et al* report on the field emission characteristics of micromachined silicon tips coated with lanthanum hexaboride by electron-beam evaporation [37]. Using molybdenum as a seed layer to promote adhesion of the LaB_6 films to the silicon tips, they conclude that the quality of the resultant films depends primarily upon the temperature of the silicon substrate (which significantly affects the stoichiometry and the crystallinity of the deposited film) and to a lesser extent on the beam evaporation power. Their results showed that when the

substrate temperature was low, the adhesion between the silicon tip surface and the LaB_6 film became poor. Investigations revealed that best results were obtained at a substrate temperature of 300°C . Okamoto *et al* [38] also used the electron-beam evaporation technique to deposit LaB_6 thin-films, but in their investigation opted to use nickel as the substrate material. They observed that the work function of the resultant film was dependant on its crystallographic orientation when deposited and achieved the lowest value of between 2.4 to 2.5 eV for the {100} orientation.

8. Heating Prior to Ignition

A heater is necessary in the hollow cathode design to raise the emitter temperature sufficiently for the generation of energetic electrons. This significantly reduces the breakdown voltage of the device when compared to a non-heated start. In conventional macro-scale devices, the heater traditionally uses refractory metals such as tungsten, molybdenum or tantalum as a resistive dissipater, typically raising the cathode temperature of the order of $\sim 1200^\circ\text{C}$. At the University of Southampton gold has been deposited around pyramidal pits etched into silicon, producing tracks ($20\mu\text{m}$ wide, $5\mu\text{m}$ thick) through which an electrical current is passed. This process, albeit with differing materials, can also be applied to the creation of heating elements on the surface of emitter structures.

A parallel heater configuration was chosen for redundancy. Individual track failure results in increased current through each track and a corresponding increase in voltage and dissipative output from each winding but not device failure. Characteristics of various materials considered are shown in Table 3.

Due to the low resistivity refractory metals, a significant reduction in heater cross sectional area is required to give the desired resistivity for parallel operation. Given the materials which are able to sustain operation $>1200^\circ\text{C}$, rhenium would be a poor choice since it possesses a high emissivity and would thus radiate a significant proportion of the input energy. Of the remaining materials, tungsten would seem to present the most favourable characteristics based on the lowest emissivity, highest melting point and highest thermal conductivity when compared against tantalum and molybdenum, hence tungsten was selected.

9. Conservative Design Solution

Several iterations were made of the design solution to distinguish more optimal configurations. Central to the design of the first microspacecraft propulsion system is to meet thrust requirements while providing a conservative design with redundancy. Since operation at high orifice current densities has not been documented a conservative design has an orifice current density no higher than conventional cathodes to date. In this case the T5 hollow cathode operates at $\sim 65\text{A}/\text{mm}^2$. Limiting the acceptable current density reduces the maximum Ohmic dissipation within the plasma. In the case of a single hollow cathode rather than array this would result in insufficient energy equipartition into the plasma to give reasonable performance and a high degree of ionization. One additional point to note is that an early design realization to reduce losses was to construct the orifice, in which the majority of energy equipartition occurs, as part of the anode. In taking this approach the device efficiency was significantly improved due to the reduction in ion recombination losses within the orifice.

To compensate for low tolerable current densities mass flow rate must be reduced to maintain the specific power invested in the flow and specific impulse while total thrust requirement can be met by additional cathodes added in an array and total mass flow increased proportionally to meet thrust requirements. A 100-cathode array presented reasonable solutions and also allowed for redundancy should an individual cathode or series of cathodes fail. Orifice diameter was selected at $10\mu\text{m}$ since this is both small enough to generate resistive dissipation at low currents and well within conventional MEMs manufacturing constraints, while orifice length was selected to be no more than twice that of the orifice diameter consistent with conventional hollow cathode design and thus set at $20\mu\text{m}$ to reduce the required discharge current.

As result of reducing mass flow rate through individual in this case to $1.5\mu\text{g}/\text{s}$ ($0.15\text{mg}/\text{s}$ total mass flow rate) the emitter diameter must be increased to maintain the pressure-cavity diameter relationship consistent with oscillatory enhancement and the hollow cathode effect. This results in a relatively low emitter pressure of 44Torr; only an order of magnitude lower than in conventional cathodes and as such results in a fairly large emitter diameter of 0.28mm for preservation of the hollow cathode effect. The array in this case required a total discharge current of 620mA ($6.2\text{mA}/\text{cathode}$) dictating that the exposed anode area required for cooling by

radiation be no less than 0.29mm^2 for operation at 1000°C or 0.57mm^2 operating at 800°C . This gives a minimum chip size of $0.75\text{mm} \times 0.75\text{mm}$ from a thermodynamic viewpoint showing that in this configuration, emitter geometry is actually the driver of chip size and cathode spacing rather than cooling requirements. In this case a 100 cathode array emitter has a theoretical minimum chip size is $2.8\text{mm} \times 2.8\text{mm}$ based on emitter geometry and more practically $5.6\text{mm} \times 5.6\text{mm}$ if allowing for spacing's between emitters to be equal to emitter diameters.

The electric field at the emitter surfaces of $1.3 \times 10^7 \text{V}/\text{m}$ due to the small Debye length (2.7pm) leads to a large reduction in effective work function from 2.50eV to 2.36eV . This is a significantly larger reduction than in conventional LaB_6 cathode and thus results in a relatively low operating temperature of only 928°C to give the 6.2mA per emitter. At this temperature it is a safe assumption that lifetime will not be limited by thermal desorption of the emitter material since LaB_6 cathodes have traditionally operated at much higher temperatures for thousands of hours.

Since the circuit is essentially parallel the total resistance is low resulting in a total voltage drop of only 9.53V at 620mA , a total array power of 5.91W , well within the resource constraints of small spacecraft. Since the current density is limited, Ohmic dissipation in individual cathodes is small which limits specific impulse $\sim 75\text{s}$ (gas temperature of 1802°C). Since electron, ionization and convective losses dominate in this case thrust efficiency is reduced to 0.68%. Total mass follow rate to meet the 0.11mN thrust requirement is 0.15mgs^{-1} which could be catered for with a conventional 2-stage bang-bang flow regulation system since upstream pressure is 5876Pa or 59mbar .

A 10-track parallel tungsten heater circuit was designed to give a total voltage drop of 24V consistent with a small satellite bus. A geometrically pleasing $5\mu\text{m}$ track with width and $1\mu\text{m}$ track height was selected which required 174mA to give the 4.19W dissipative power in the heater for ignition, the total circuit resistance being 138Ω . Each heater track required 34 cross-chip windings to give the necessary voltage parameters by increasing resistivity; in this case covering an acceptable 17% of the rear face of the chip. Two MEMS manufacturable configurations of these cathodes are shown in Figure 4.

10. Conclusion

An initial feasibility study into the scaling of hollow cathode devices to operate as an electrothermal thruster at micrometer scale has been presented. Although some design requirements are indeed challenging there do not seem to be any critical issues regarding the production and operation of hollow cathode devices at this scale which would fundamentally limit the application of the technology. A very conservative design exercise yielded a device able to operate at less than 6-Watts which would be suited to the performance requirements of a 20kg spacecraft at approximately 75s specific impulse. If such a device can be realized with these performance parameters small spacecraft missions may be able to significantly benefit from this technology. An attempt to manufacture the device at the University of Southampton is planned in the near future.

11. References

- [1] A.N. Grubisic and SB Gabriel, Characterization of the T-series hollow cathode thrusters for all-electric spacecraft, IEPC-2007-81, International Electric Propulsion Conference, Florence, Italy, (2007).
- [2] A.N. Grubisic and SB Gabriel, Hollow cathode thrusters for all-electric spacecraft, IAC-07-C4.4.07, 58th International Astronautical Federation Congress, Hyderabad, India, (2007).
- [3] S Pottinger, P Gessini, D Webb, R Intini Marques and SB Gabriel, Electric propulsion research at the University of Southampton, Journal of the British Interplanetary Society, 59(5), (2006).
- [4] P Gessini, SB Gabriel and DG Fearn, Thrust characterization of a T6 hollow cathode, IEPC Paper 05-257, 29th International Electric Propulsion Conference, Princeton, NJ, (2005).
- [5] P Gessini, SB Gabriel and DG Fearn, The T6 hollow cathode as a microthruster, AIAA Paper 2005-4078, 41st AIAA/ASME/SAE/ASEE Joint Propulsion Conference & Exhibit, Tucson, AZ, (2005).
- [6] HL Gray, *Development of ion propulsion systems*, GEC Rev., 12(3), 154-168 (1997)
- [7] NC Wallace and DG Fearn, The design and performance of the T6 ion thruster, American Institute of Aeronautics and Astronautics, Paper 98-3342, (1998).
- [8] D Fearn, A Singfield, N Wallace, S Gab and P Harris, The operation of ion thruster hollow cathodes using rare gas propellants, AIAA Paper 90-2584, (1990).
- [9] PM Latham, AR Martin and A Bond, Design, manufacture and performance of the UK-25 engineering model thruster, AIAA Paper 90-2541, (1990).
- [10] PT Harris and S Gair, A review of the cathode construction for the RAE 10/25 mN thruster, IEPC Paper 88-078, (1988).
- [11] CM Philip and DG Fearn, Recent hollow cathode investigations at the Royal Aircraft Establishment, AIAA paper 73-1137, AIAA J, 12, 10, 1319-25, 1974.
- [12] DG Fearn, The operation of hollow cathodes under conditions suitable for ion beam neutralization, IEE Conf. Pub., 100, 146-150 (1973).
- [13] JL Cronin, Modern dispenser cathodes, IEEE Proc., 128, 19-32 (1981).
- [14] RA Martin, Atomic excitation processes in the discharge of rare gas ion-engines, J. Phys. BLAtom. Molec. Phys., 7(10), (1974).
- [15] L Spitzer Jr., 'Physics of fully ionized gases', Interscience Publishers Inc., New York, (1956).
- [17] Germer L H 1959 J. Appl. Phys. 30 46
- [18] AD White, J. Appl. Phys., 30, 711 (1959).
- [19] DJ Sturges and HJ Oskam, J. Appl. Phys., 35, 2887 (1964).
- [20] KH Schoenbach, R Verhappen, T Tessnow, PF Peterkin and W Byszewski, Appl. Phys. Lett., 68, 13 (1996).
- [21] YB Guo and FCN Hong, Appl. Phys. Lett., 82, 337 (2003).
- [22] C Penache, A Braeuning-Demian, L Spielberger and H Schmidt-Boecking, Proc. of the Hakone VII, Greifswald, Germany, 2, 501 (2000).
- [23] JW Frame and JG Eden, Electr. Lett., 34, 1529 (1998).
- [24] JG Eden, SJ Park, NP Ostrom, ST McCain, CJ Wagner, BA Vojak, J Chen, C Liu, P von Allmen, F Zenhausern, DJ Sadler, J Jensen, DL Wilcox and JJ Ewing, J. Phys. D, 36, 2869 (2003).
- [25] W Shi, RH Stark and KH Schoenbach, IEEE Trans. Plasma Sci., 27, 16 (1999).
- [26] P von Allmen, DJ Sadler, C Jensen, NP Ostrom, ST McCain, BA Vojak and JG Eden, Appl. Phys. Lett., 82, 4447 (2003).
- [27] P von Allmen, ST McCain, NP Ostrom, BA Vojak, JG Eden, F Zenhausern, C Jensen and M Oliver, Appl. Phys. Lett., 82, 2562 (2003).
- [28] A Fiala, LC Pitchford and JP Boeuf, Two-dimensional, hybrid model of glow discharge in hollow cathode geometries, Proc. XXII Conf. Phenomena in Ionized Gases, Hoboken, NJ, 4, 191 (1995).
- [29] L Stenmark, M Lang, J Köhler, and U Simu, Micromachined propulsion components, Proc. 2nd Round Table on Micro/Nano Technologies for Space, ESTEC, Noordwijk, The Netherlands, ESA WPP-132, 69-76 (1997).
- [30] J Mueller, S Vargo, A Green, D Bame, R Orens and L Roe, Development of a micro-isolation valve: Minimum energy requirements, repeatability of valve actuation and preliminary studies of debris generation, AIAA Paper 2000-3675, 36th Joint Propulsion Conference, Huntsville, AL, (2000).
- [31] M Koch, N Harris, AGR Evans, NM White and A Brunnschweiler, A novel micromachined pump based on thick-film piezoelectric actuation, Sensors and Actuators A, 70(1-2), 98-103 (1998).
- [32] C Haas and M Kraft, Low-cost fabrication of valveless micropumps, Proc. MME 2006 Conference, UK, 65-68 (2006).
- [33] CGJ Schabmueller, Self-aligning gas/liquid micropump J. Micromech. Microeng., 12, 420-424 (2002).
- [34] CGJ Schabmueller, M Koch, AGR Evans and A Brunnschweiler, Design and fabrication of a microfluidic circuitboard, J. Micromech. Microeng., 9, (1999).
- [35] DM Goebel and RM Watkins, LaB₆ hollow cathodes for ion and Hall thrusters, AIAA-2005-4239, 41st Joint Propulsion Conference,

Tucson, AZ, (2005).

[36] JG Eden and SJ Park, Microcavity plasma devices and arrays: a new realm of plasma physics and photonic applications, Plasma Phys. Control. Fusion, 47, 83–92 (2005).

[37] X Wang, Z Lin, K Qi, Z Chen, Z Wang and YJiang, Field emission characteristics of lanthanum hexaboride coated silicon field emitters, J. Phys. D: Appl. Phys., 40, 4775-4778 (2007).

[38] Y Okamoto, T Aida and S Shinada, DC gas-discharge display panel with LaB₆ thin-film cathode, Japan J. Appl. Phys., 26(10), 1722-1726 (1987).

S/C Dimensions Mass (kg)	Scale (m)	Moment of Inertia (kgm ²)	Required Impulse Bit (Ns)						Min. Thrust for slew (mN)
			17mrad		0.3mrad		0.02mrad		
			20s	100s	20s	100s	20s	100s	
1	0.1	0.017	1.4×10^{-4}	2.9×10^{-5}	2.5×10^{-6}	5.1×10^{-7}	1.7×10^{-7}	3.4×10^{-8}	0.014
10	0.3	0.150	4.3×10^{-4}	8.5×10^{-5}	7.5×10^{-6}	3.0×10^{-6}	1.0×10^{-6}	1.0×10^{-7}	0.043
20	0.4	0.533	1.1×10^{-3}	2.3×10^{-4}	2.0×10^{-5}	4.0×10^{-6}	1.3×10^{-6}	2.7×10^{-7}	0.110

Table 1: Representative thrust requirements for micro-spacecraft [30].

Propellant	Mercury	Caesium	Xenon	Krypton	Argon
Atomic number	80	55	54	36	18
Atomic mass [g.mol ⁻¹]	200.59	132.90	131.29	83.80	39.95
Density at 20°C 1Bar [g.cm ⁻³]	13.6	1.9	5.9	3.73	1.78
Boiling point [°C]	356	669	-107	-153	-185
Energy of first ionisation [kJ.mol ⁻¹]	1796	375	1170	1351	1520
Energy of second ionisation [kJ.mol ⁻¹]	3294	2234	2046	2350.4	2665

Table 2: Propellant Characteristics.

Material Properties	Gold	Silicon	Tungsten	Tantalum	Molybdenum	Rhenium
Electrical resistivity 20°C [Ohm-m]	2.2×10^{-8}	1.0×10^{-4}	6.7×10^{-8}	1.3×10^{-7}	5.7×10^{-8}	1.9×10^{-7}
Electrical resistivity 1200°C [Ohm-m]	NA	NA	4.03×10^{-7}	6.30×10^{-7}	3.84×10^{-7}	8.44×10^{-7}
Thermal conductivity [W/m-K]	301	124	163	54	138	40
Emissivity	0.04	0.3-0.5	0.15	0.2	0.17	0.42
Density [g/cm ³]	19.32	2.3	19.3	16.65	10.22	21.03
Melting point [C]	1064	1412	3370	2996	2617	3180

Table 3: Material properties for heater selection

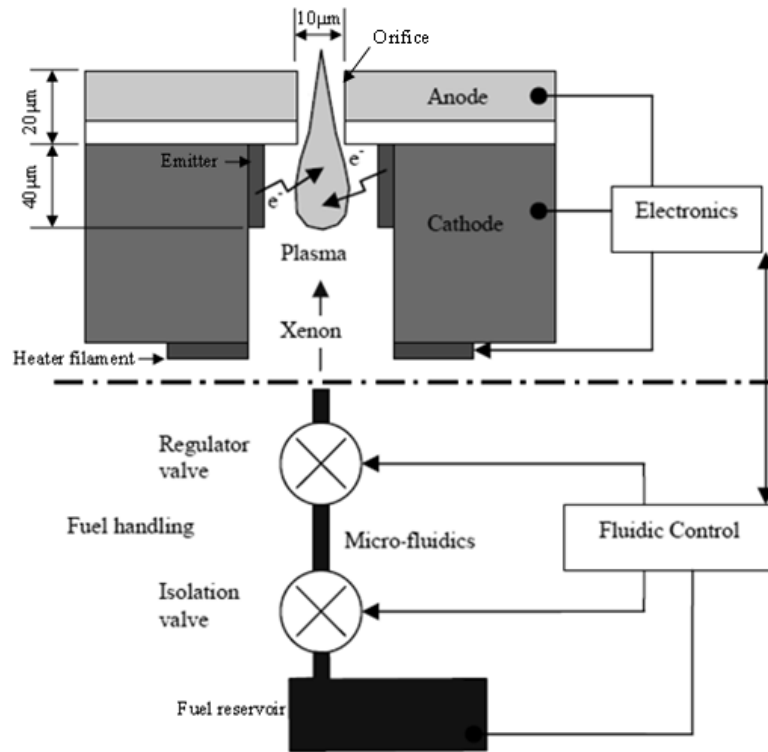


Figure 1: Thruster design layout – not to scale

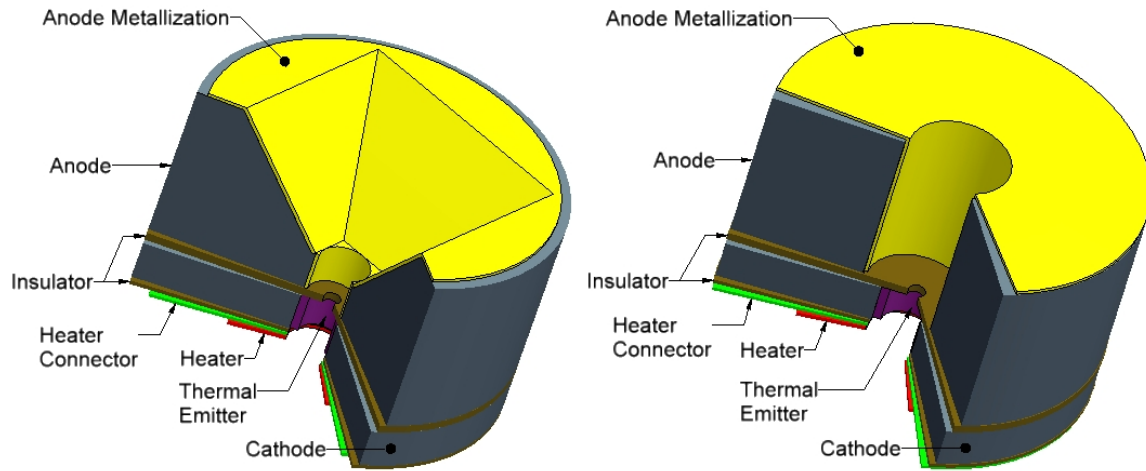


Figure 2: Various conceived configurations based on a silicon substrate